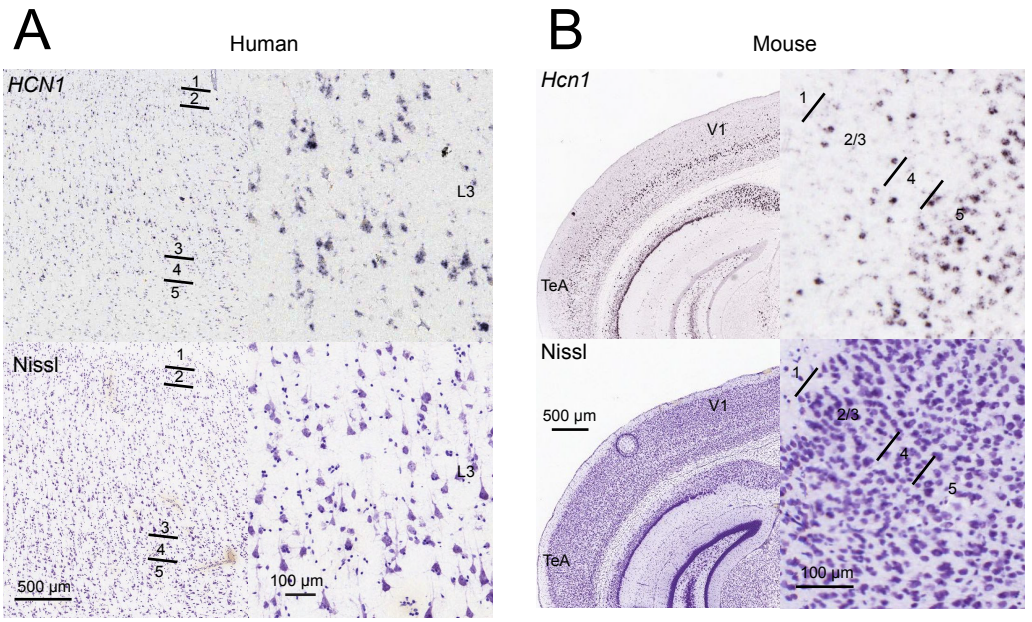
A
Human
HCN1
1
2
L3
3
4
5
Nissl
500 µm
100 µm
B
Mouse
Hcn1
V1
TeA
1
2/3
4
5
Nissl
500 µm
100 µm

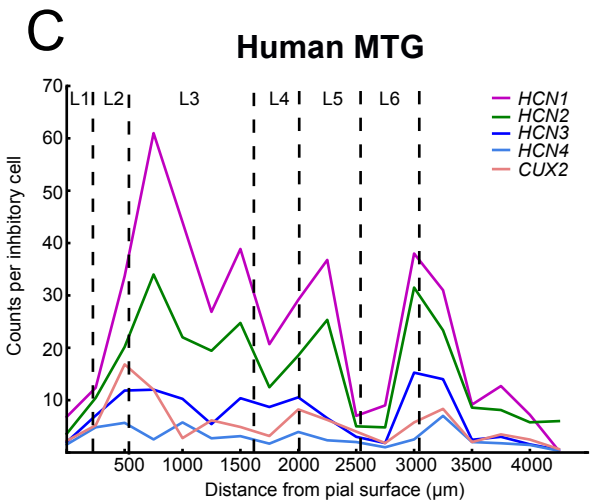
C
Human MTG
L1
L2
L3
L4
L5
L6
HCN1
HCN2
HCN3
HCN4
CUX2
Counts per inhbitory cell
Distance from pial surface (µm)

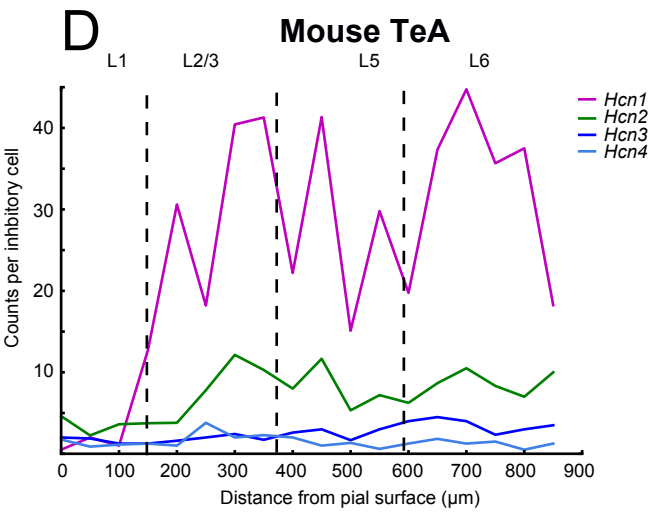
D
Mouse TeA
L1
L2/3
L5
L6
Hcn1
Hcn2
Hcn3
Hcn4
Counts per inhbitory cell
Distance from pial surface (µm)

Figure S1- H-channel Related Gene Expression in Mouse Versus Human Cortex, Related to Figure 1. A) ISH of *HCN1* in human temporal cortex at low magnification (left column, with near adjacent Nissl stained section for layer identification) and high magnification in deep L3. **B)** ISH of *Hcn1* in mouse neocortex at low magnification (left column, with near adjacent Nissl stained section) and high magnification of TeA. Single RNA-counts per *GAD2*+ cell from mFISH data for **C)** human MTG and **D)** mouse TeA. *CUX2* was used to identify L2 and 3 in human cortex. *GAD2* was used to identify inhibitory cells.

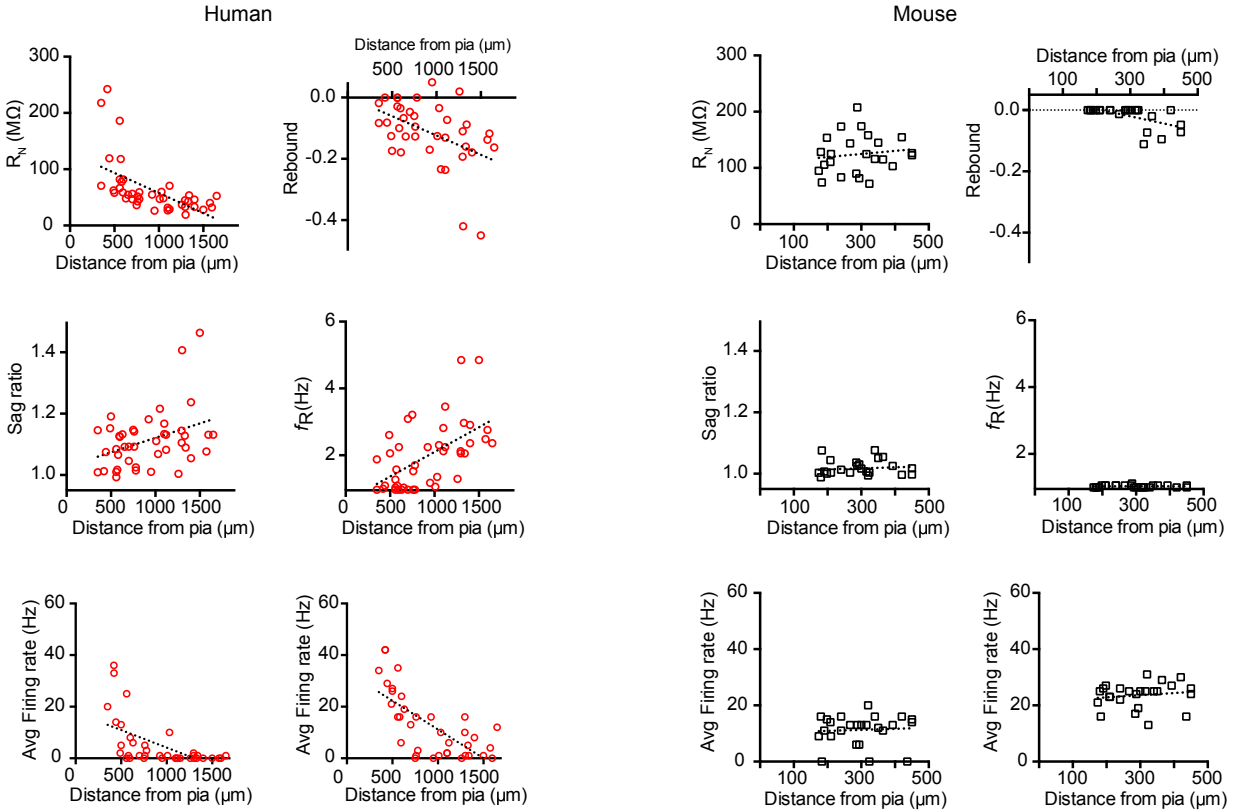
Human
Mouse
R_N (MΩ)
Rebound
Distance from pia (μm)
Sag ratio
f_R(Hz)
Avg Firing rate (Hz)
0
500
1000
1500
100
300
500
-0.4
-0.2
0.0
1.0
1.2
1.4
2
4
6
20
40
60
200
100
300

Figure S2- Intrinsic Membrane Properties of Human (left) and Mouse (right) Supragranular Pyramidal Neurons at a Common Membrane Potential -65 mV, Related to Figure 2-5. For human, R_N (r^2 = 0.32, p < .001), rebound (r^2 = 0.22, p = .003), sag (r^2 = 0.14, p = .014), resonant frequency (r^2 = 0.32, p < .001), number of spikes in response to 250 pA (r^2 = 0.33, p < .001) and 500 pA (r^2 = 0.49, p < .001) were all significantly correlated with somatic depth from pia when measured from a common membrane potential of -65 mV. For mouse R_N (r^2 = 0.02, p = 0.53), sag (r^2 < 0.01, p = 0.65), resonant frequency (r^2 < 0.01, p = 0.99), number of spikes in response to 250 pA (r^2 < 0.01, p = 0.77) and 500 pA (r^2 = 0.02, p = 0.47) were not significantly correlated with somatic depth from pia when measured from a common membrane potential of -65 mV. Only rebound was correlated with depth from pia (r^2 = 0.35, p = 0.002).

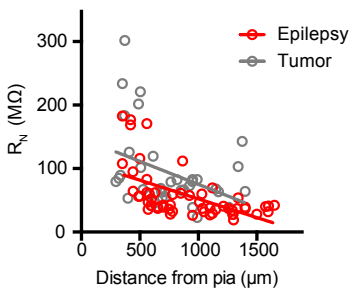
Epilepsy
Tumor
300
200
100
0
R_N (MΩ)
0
500
1000
1500
Distance from pia (µm)

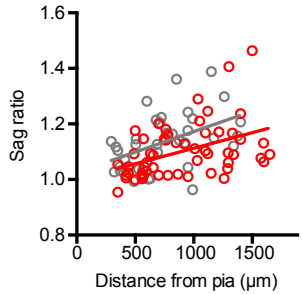
1.6
1.4
1.2
1.0
0.8
Sag ratio
0
500
1000
1500
Distance from pia (µm)

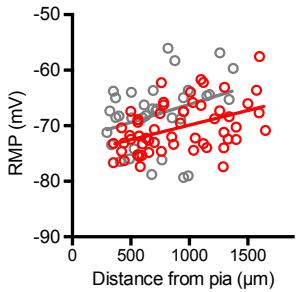
-50
-60
-70
-80
-90
RMP (mV)
0
500
1000
1500
Distance from pia (µm)

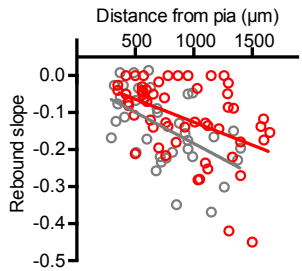
Distance from pia (µm)
500
1000
1500
0.0
-0.1
-0.2
-0.3
-0.4
-0.5
Rebound slope

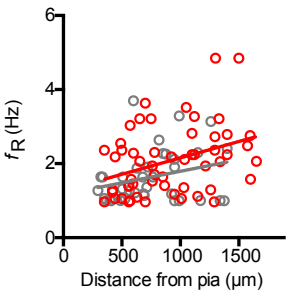
6
4
2
0
f_R (Hz)
0
500
1000
1500
Distance from pia (µm)

Figure S3- Comparison of Intrinsic Membrane Properties of Supragranular Pyramidal Neurons from Epilepsy Versus Tumor Patients, Related to Figures 2-4. For tumor patients, R_N (r^2 = 0.14, p = 0.02), sag ratio (r^2 = 0.21, p = 0.004), RMP (r^2 = 0.11, p = 0.046) and rebound (r^2 = 0.29, p < 0.001) were all significantly correlated with somatic distance from the pial surface. The correlation for resonance was not statistically significant (r^2 = 0.08, p = 0.105). The slopes of the linear fit for R_N, sag ratio, RMP, rebound and resonance were not significantly different between tumor and epilepsy patients (for all features p > 0.44, ANCOVA). However, the y-intercepts for each linear fit depended on the disease state (for all features p < 0.02, ANCOVA) for all features but resonance (p = 0.08, ANCOVA). n=38 cells from 5 donors.

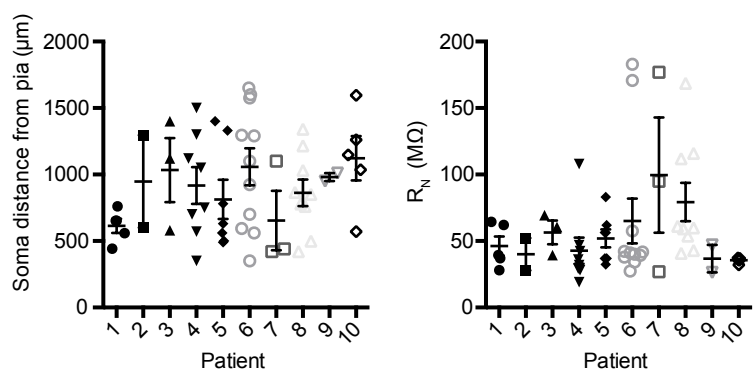
Soma distance from pia (µm)
2000
1500
1000
500
0
1 2 3 4 5 6 7 8 9 10
Patient

R_N (MΩ)
200
150
100
50
0
1 2 3 4 5 6 7 8 9 10
Patient

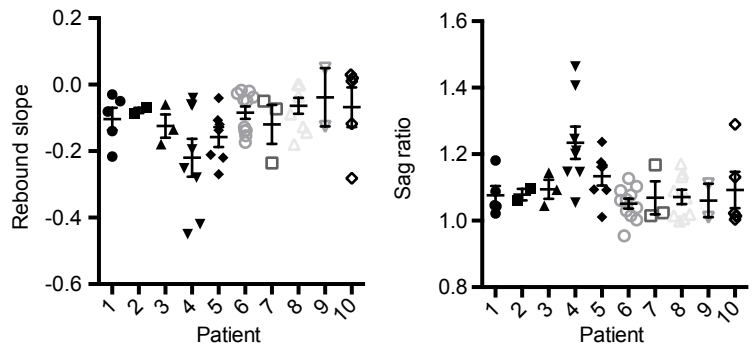
Rebound slope
0.2
0.0
-0.2
-0.4
-0.6
1 2 3 4 5 6 7 8 9 10
Patient

Sag ratio
1.6
1.4
1.2
1.0
0.8
1 2 3 4 5 6 7 8 9 10
Patient

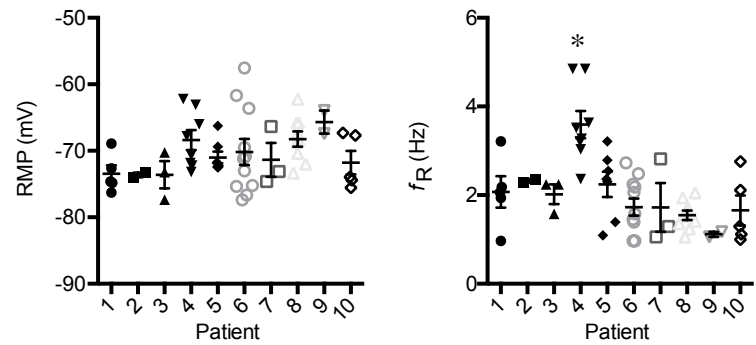
RMP (mV)
-50
-60
-70
-80
-90
1 2 3 4 5 6 7 8 9 10
Patient

f_R (Hz)
6
4
2
0
*
1 2 3 4 5 6 7 8 9 10
Patient

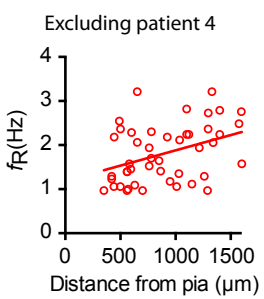
Excluding patient 4
f_R(Hz)
4
3
2
1
0
0 500 1000 1500
Distance from pia (µm)

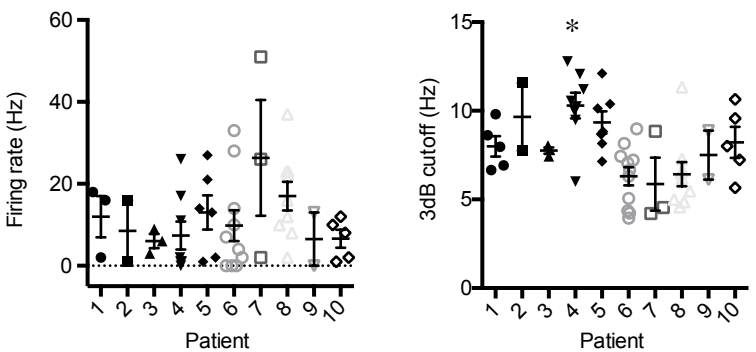
Firing rate (Hz)
60
40
20
0
1 2 3 4 5 6 7 8 9 10
Patient

3dB cutoff (Hz)
15
10
5
0
*
1 2 3 4 5 6 7 8 9 10
Patient

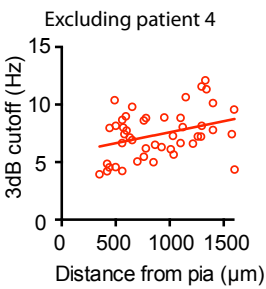
Excluding patient 4
3dB cutoff (Hz)
15
10
5
0
0 500 1000 1500
Distance from pia (µm)

Figure S4- h-Channel-related membrane properties as a function of patient, Related to Figures 2-5. Data points are plotted as a function of patient and are presented as mean ± SEM. There were no statistical differences between patients in the somatic distance from the pial surface, R_N, rebound slope, RMP and firing rate to a 500 pA current injection (all p values > 0.05, Kruskal-Wallis test). Resonant frequency and cutoff frequency were higher in neurons recorded from patient 4 compared with other patients ($p < 0.05$ Kruskal-Wallis test followed by Dunn's multiple comparisons test). However, excluding these data points still resulted in significant correlations of resonance ($r^2 = 0.16$, $p = 0.005$) and cutoff ($r^2 = 0.12$, $p = 0.02$) with somatic distance from the pial surface (plots shown at right).

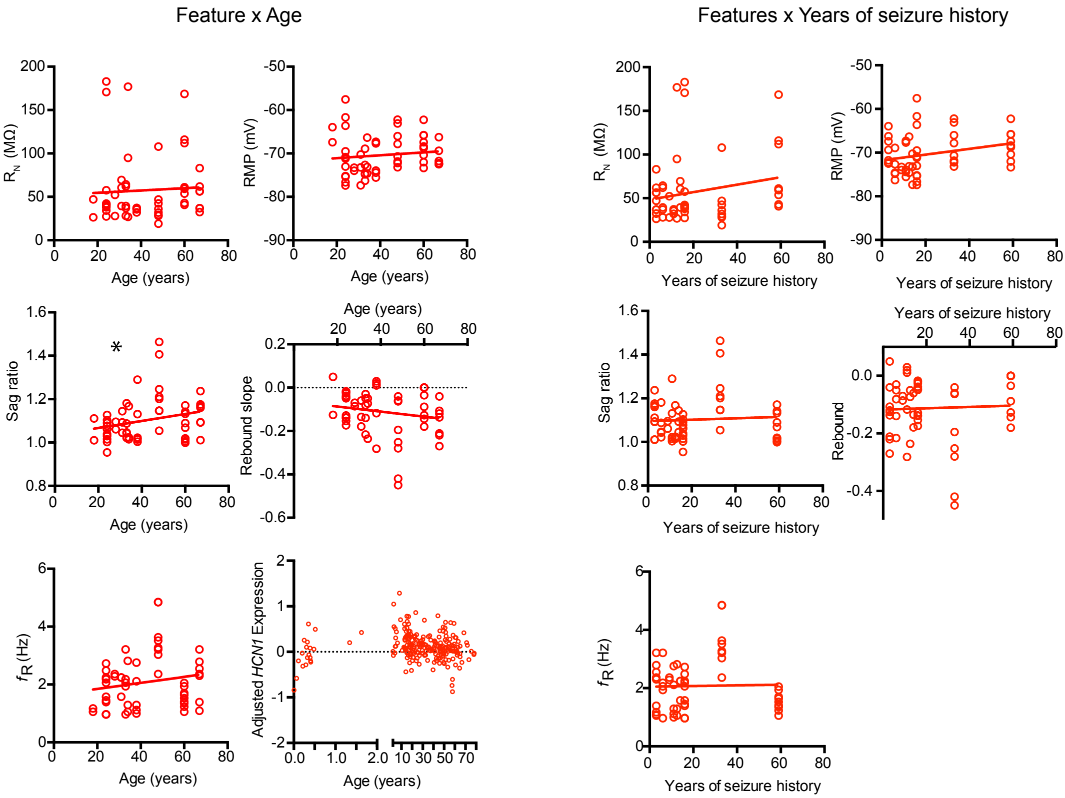

Feature x Age
Features x Years of seizure history
R_N (MΩ)
RMP (mV)
Age (years)
Years of seizure history
Sag ratio
*
Rebound slope
Rebound
f_R (Hz)
Adjusted *HCN1* Expression

Figure S5- I_h-related Membrane Properties as a Function of Patient Age and Years of Seizure History, Related to Figures 2-4. All correlations (Spearman's r) were non-significant ($p > 0.07$) with the exception of sag as a function of age ($p = 0.035$). Also, *HCN1* expression from braincloud.jhmi.edu (Colantuoni et al., 2011) is plotted as a function of age.

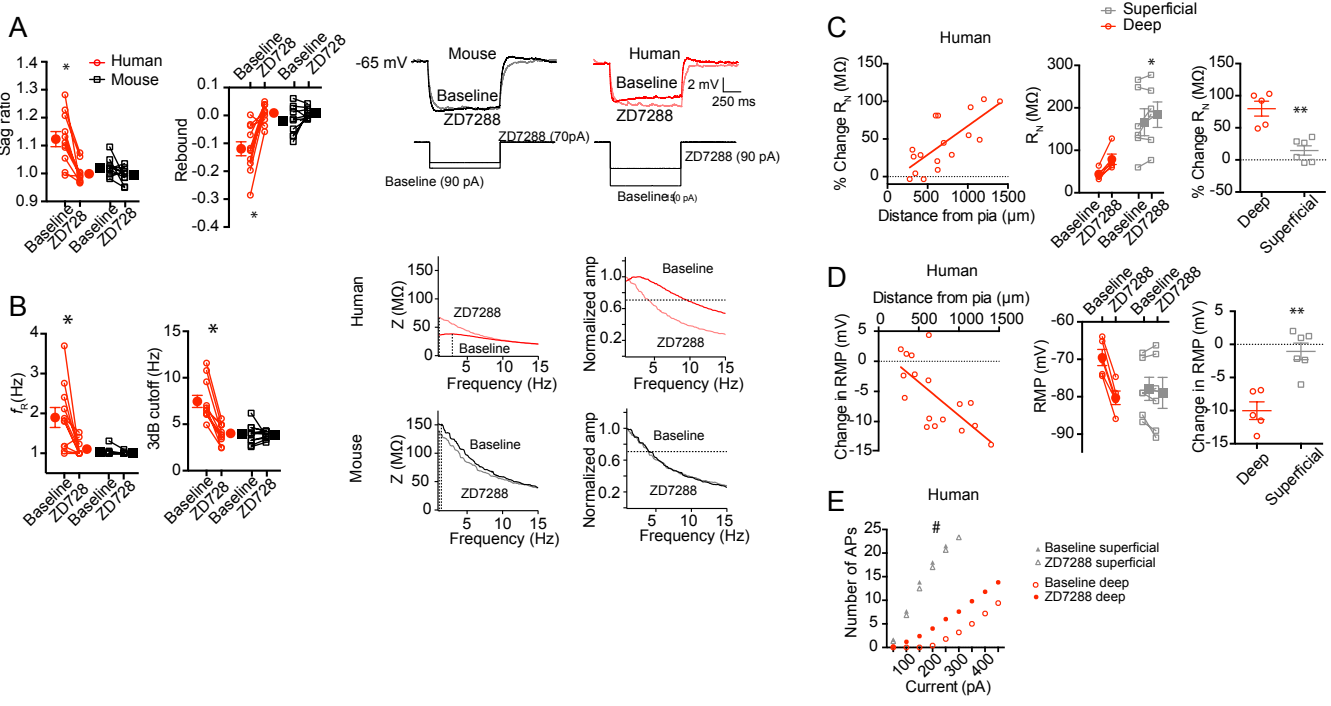
A
Human
Mouse
Sag ratio
Rebound
Baseline
ZD728
-65 mV
Mouse
Baseline
ZD7288
ZD7288 (70pA)
Baseline (90 pA)
ZD7288 (90 pA)
Human
2 mV
250 ms
B
f_R (Hz)
3dB cutoff (Hz)
Human
Mouse
Z (MΩ)
Frequency (Hz)
Normalized amp
C
Superficial
Deep
% Change R_N (MΩ)
Distance from pia (μm)
R_N (MΩ)
D
Change in RMP (mV)
RMP (mV)
E
Number of APs
Current (pA)
Baseline superficial
ZD7288 superficial
Baseline deep
ZD7288 deep

Figure S6- The Effect of ZD7288 on Intrinsic Membrane Properties of Supragranular Pyramidal Neurons in Mouse and Human Cortex, Related to Figure 6. A) Sag and rebound before and after the application of 10 μM ZD7288. Example voltage responses before and after application of ZD7288 are also shown. * $p < 0.01$, Bonferroni's post-hoc comparison. B) Resonance and 3dB cutoff before and after application of ZD7288. Example ZAPs and normalized frequency response curves before and after application of ZD7288 are also shown. * $p < 0.01$, Bonferroni's post-hoc comparison. C) Effect of ZD7288 on intrinsic membrane properties as a function somatic distance from pial surface in human cortex. The percent change in R_N after application of ZD7288 correlated with somatic depth from the pial surface (n = 17 cells from 6 donors, $r^2 = 0.55$, $p < 0.001$). In the presence of ZD7288, deep (soma > 1000 μm from pial surface, n = 5 cells from 3 donors) supragranular neurons had a lower R_N than superficial neurons (soma < 500 μm from pial surface, n = 6 from 2 donors; $p < 0.001$ Mixed ANOVA; * $p < 0.025$ Bonferroni's post-hoc comparison of R_N). The R_N of deep neurons increased by a greater percentage than superficial neurons upon application of ZD7288 (** $p < 0.001$, t-test). D) The change in RMP after application of ZD7288 correlated with somatic depth from the pial surface in human cortex ($r^2 = 0.48$, $p = 0.002$). RMP in the presence of ZD7288 was equal for deep and superficial neurons ($p > 0.05$, Bonferroni's post hoc comparison). Deep neurons hyperpolarized more than superficial neurons upon application of ZD7288 (** $p < 0.001$, t-test). E) FI curves for superficial and

deep neurons in human cortex were different in the presence of ZD7288 (# p <0.001, Mixed-ANOVA). Filled symbols represent mean ± SEM.

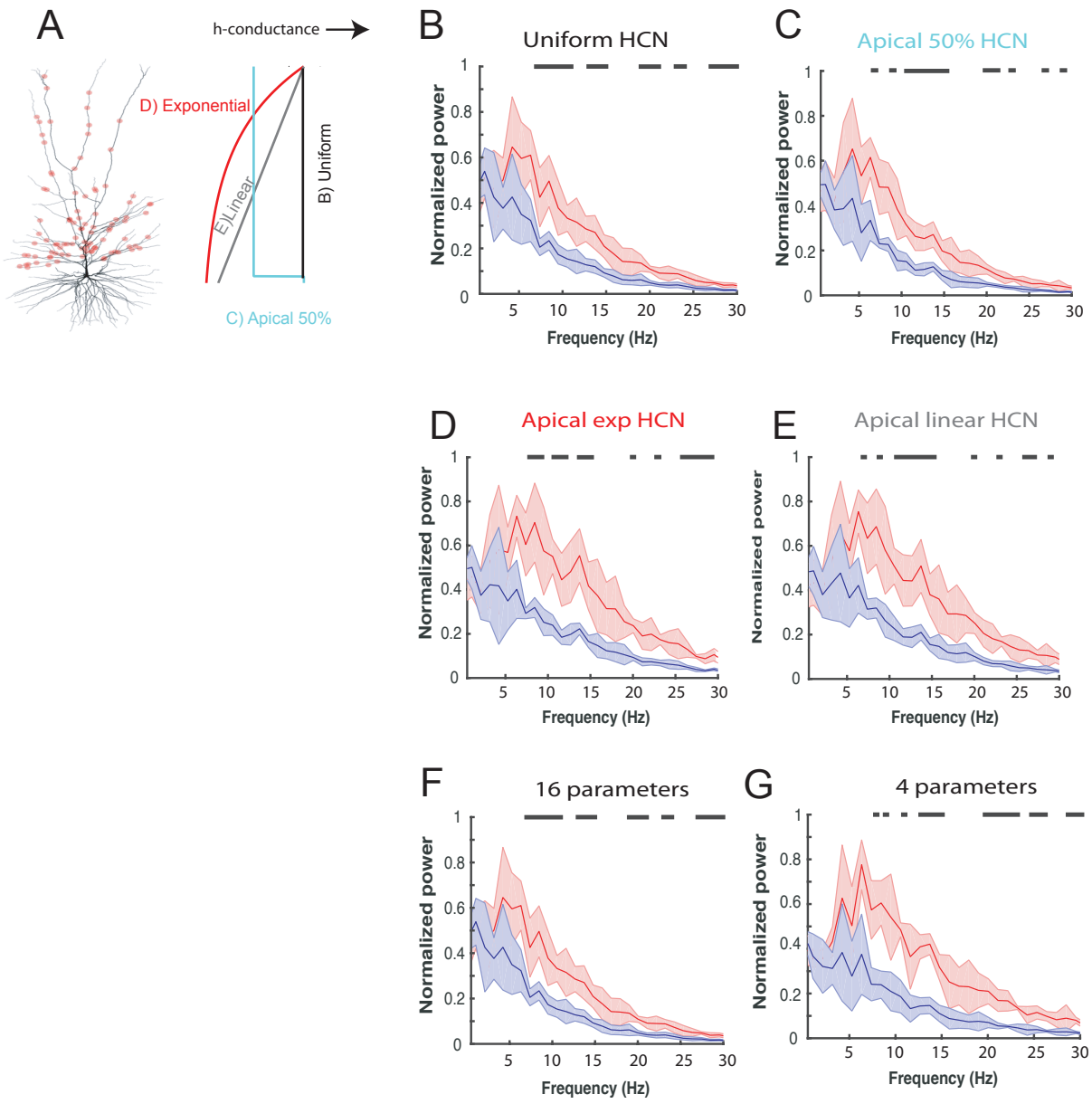
A
h-conductance
D) Exponential
E) Linear
B) Uniform
C) Apical 50%
B
Uniform HCN
C
Apical 50% HCN
D
Apical exp HCN
E
Apical linear HCN
F
16 parameters
G
4 parameters
Normalized power
Frequency (Hz)

Figure S7- Enhancement of Theta-band Signals in Somatic Membrane Potential is Robust to Different Gradients of I_h and Constrained Passive Parameters, Related to Figure 7. Power spectrum of the somatic membrane potential of the I_h(+) and I_h(-) model when stimulated by 1000 synapses randomly located along the apical dendrite with various distributions (A) of HCN expression and passive membrane parameter models. B) Original model with uniform h-channel density. C) Model with 50% less somatic HCN density than the original model. D) Model with exponentially increasing HCN density, $g_{HCN} = (2.849e - 07) * (-0.869 + 2.087 * \exp(0.003 * distance))$. E) Model with linearly increasing HCN density, $g_{HCN} = (3.427e - 07) * (1.217 + 0.007 * distance)$. Black stripes correspond to the statistically significant differences in normalized power spectrums after correction for multiple comparisons using Bonferroni correction. Inset: location of a subset (100 out of 1000) synapses is shown as well as schematic of different h-channel gradients tested. F) The original model with 16 passive parameters, the same as in Fig. 7 H. G) A model with 4 passive parameters matched in all compartments. Black stripes correspond to the statistically significant differences in normalized power spectrums after correction for multiple comparisons using Bonferroni correction. Data are presented as mean ± SD.

Age (years)	Sex	Years of Seizure History	Diagnosis	Antiepileptic drugs	Resection location
33	F	6	Cavernoma	GPN, LSC, LTG, LEV, TPM	R-temporal lobe
28	F	9	TLE	LSC, LTG	L-temporal lobe
31	M	14	TLE	CBZ, LRZ	R-temporal lobe
48	F	33	TLE	LEV, LTG, LRZ, ZON, PHN	L-temporal lobe
67	M	3	TLE	LEV, LSC, TGB, LTG,	L-temporal lobe
24	F	16	TLE	LRZ, OXZ	R-temporal lobe
34	F	12.5	TLE	LEV, LTG	L-temporal lobe
60	M	59	TLE	PHT, CBZ, LTG, LEV, GPN, PB, PRM	R-temporal lobe
18	M	3	TLE	PMP, GPN, LRZ,	R-temporal lobe
38	F	11	TLE	LEV, TPM	L-temporal lobe
47	M	<1	Tumor	LEV	L-frontal
68	F	0	Lesion		R-temporal
57	F	0	Tumor		L-temporal lobe
25	M	<1	Tumor	LEV	R-temporal lobe

23	F	10	TLE	LSC, LTG, LRZ	R-temporal lobe
40	M	5	TLE	VPA, LSC, CZP	R-temporal
68	F	0	Tumor		Frontal

CBZ, Carbamazepine; GPN, Gabapentin; LSC, Lacosamide; LTG, Lamotrigine; LEV, Levetiracetam; LRZ, Lorazepam; OXZ, Oxcarbazepine; PB, Phenobarbital; PMP, Perapanel; PRM, Primidone; TGB, Tiagabine; TPM, Topiramate; ZON, Zonisamide; PHN, Phenytoin; VPA, Valproic acid; CZP, Clonazepam

Table S1 – Patient information, Related to STAR Methods